Synthesis, X-ray, and NMR Studies on Palladium BINAP Complexes Containing Oxazolidinone and Acetylacetonate Anions

Devendrababu Nama and Paul S. Pregosin*

Laboratory of Inorganic Chemistry, ETHZ, 8093 Zürich, Switzerland

Alberto Albinati* and Silvia Rizzato

Department of Structural Chemistry (DCSSI), University of Milan, 20133 Milan, Italy

Received January 8, 2007

A series of monocationic palladium BINAP complexes, [Pd(*rac*-BINAP)(an oxazolidinone anion)][X] and [Pd(*rac*-BINAP)(an acetylacetonate anion)][X] (X = **a**, $CF_3SO_3^-$; **b**, BF_4^-) (**9**−**13**), have been synthesized and characterized. A dicationic intermediate, pertinent to the Pd-catalyzed hydroamination reaction, arising from the reaction of the bis-aquo complex $[Pd(H_2O)_2(rac\text{-BINAP})]_2(CF_3SO_3)_2$ and 1 equiv of an oxazolidinone, has been characterized via low-temperature NMR studies. The structures of the complexes $[Pd(rac\text{-BINAP})(CH_3{-}C(O){-}C(CH_3){-}C(O){-}CH_3)](BF_4)$, **12b**, and $[Pd(\mu\text{-OH})(rac\text{-BINAP})]_2(CF_3SO_3)_2$ have been determined by X-ray diffraction. The solid-state structures of *two* separate forms of the BF_4^- salt **12b** were obtained. One form of the salt can be thought of as a tight ion pair, whereas the second form contains a dichloromethane solvent molecule, packed in approximately a fifth coordination position together with a relatively remote BF_4^- anion. These structures represent a rare example where *both* ion pairing and strong solvation could be individually characterized. PGSE diffusion coefficients (*D* values) were measured for both the $CF_3SO_3^-$ and BF_4^- salts of **9**−**13** in CD_2Cl_2. In addition, *D* values were obtained for the $CF_3SO_3^-$ salts in THF and $CDCl_3$ solutions. The amount of ion pairing decreases in the sequence $CDCl_3$ > THF > CD_2Cl_2. The $^1H,^{19}F$-HOESY spectra for the salts in $CDCl_3$ suggest that the $CF_3SO_3^-$ is approaching the positive metal and phosphorus centers via a pathway that brings it closest to the P-phenyl groups but remote from the chelating anion.

Introduction

Mono- and/or dicationic Pd(II) salts play an important role in a number of catalytic transformations, e.g., allylic alkylation,[1] aldol condensation,[2] ene-type Michael additions,[3] and selected hydroamination reactions.[4] Recently, Sodeoka and co-workers,[5] and later Hii and co-workers,[6] have made extensive use of palladium(II) BINAP complexes as catalyst precursors. For the enantioselective Michael reaction using 1,3-diketones as substrates, Sodeoka[7] has generated the monocationic palladium *tert*-butyl-substituted enolate, A, shown, and found this salt to be a fairly stable intermediate. This type of chiral palladium complex is also relevant in the area of catalytic enantioselective fluorination. Li and Hii,[6b] in their studies on Pd(BINAP)-catalyzed hydroamination reactions, using unsaturated oxazolidinones as reagents, consider the dicationic chelating intermediate, B, shown above, as potentially relevant. Jorgensen and co-workers[8] have proposed a related dicationic oxazolidinone complex of nickel.

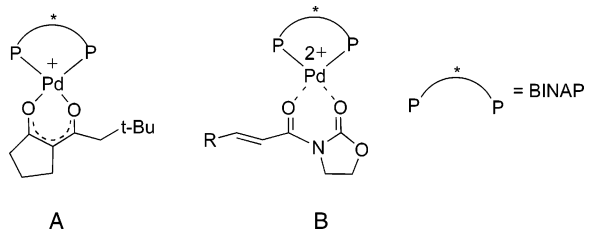

It is now fairly normal to use a number of different anions in cationic palladium chemistry. Occasionally, there are reports suggesting that the anion may play a specific role,[9−14] e.g., in

(1) Trost, B. M.; Crawley, M. L. *Chem. Rev.* **2003**, *103*, 2921−2943.
(2) Kleij, A. W.; Gebbink, R.; van den Nieuwenhuijzen, P. A. J.; Kooijman, H.; Lutz, M.; Spek, A. L.; van Koten, G. *Organometallics* **2001**, *20*, 634−647. Nesper, R.; Pregosin, P. S.; Puntener, K.; Wörle, M. *Helv. Chim. Acta* **1993**, *76*, 2239−2249.
(3) Phua, P. H.; White, J. P.; de Vries, J. G.; Hii, K. K. *Adv. Synth. Catal.* **2006**, *348*, 587−592. Ogasawara, M.; Yoshida, K.; Hayashi, T. *Organometallics* **2000**, *19*, 1567−1571.
(4) Hartwig, J. F. *Pure Appl. Chem.* **2004**, *76*, 507−516.
(5) (a). Hamashima, Y.; Takano, H.; Hotta, D.; Sodeoka, M. *Org. Lett.* **2003**, *5*, 3225−3228. (b) Hamashima, Y.; Hotta, D.; Umebayashi, N.; Tsuchiya, Y.; Suzuki, T.; Sodeoka, M. *Adv. Synth. Catal.* **2005**, *347*, 1576−1586.
(6) (a) Li, K. L.; Horton, P. N.; Hursthouse, M. B.; Hii, K. K. *J. Organomet. Chem.* **2003**, *665*, 250−257. (b) Li K. L.; Hii, K. K. *Chem. Commun.* **2003**, 1132−1133. (c) Phua, P. H.; de Vries, J. G.; Hii, K. K. *Adv. Synth. Catal.* **2005**, *347*, 1775−1780. (d) Li, K. L.; Phua, P. H.; Hii, K. K. *Tetrahedron* **2005**, *61*, 6237−6242.
(7) (a) Hamashima, D.;. Sodeoka, M. *Chem. Rec.* **2004**, *4*, 231−242. (b) Hamashima, Y.; Hotta, D.; Sodeoka, M. *J. Am. Chem. Soc.* **2002**, *124*, 11240−11241. (c) Fujii, A.; Hagiwara, E.; Sodeoka, E. M. *J. Am. Chem. Soc.* **1999**, *121*, 5450−5458.
(8) Zhuang, W.; Hazell, R. G.; Jørgensen, K. A. *Chem. Commun.* **2001**, 1240−1241. See also: Evans, D. A.; Thomson, R. J.; Franco, F. *J. Am. Chem. Soc.* **2005**, *127*, 10816−10817, for a related structure as a nickel complex.
(9) Fagnou, K.; Lautens, M. *Angew. Chem., Int. Ed.* **2002**, *41*, 27−47. Lautens, M.; Fagnou, K.; Yang, D. Q. *J. Am. Chem. Soc.* **2003**, *125*, 14884−14892.
(10) Krossing, I.; Raabe, I. *Angew. Chem., Int. Ed.* **2004**, *43*, 2066−2090.
(11) Drago, D.; Pregosin, P. S.; Pfaltz, A. *Chem. Commun.* **2002**, 286−287.
(12) Firestone, M. A.; Rickert, P. G.; Seifert, S.; Dietz, M. L. *Inorg. Chim. Acta* **2004**, *357*, 3991−3998.
(13) Lancaster, N. L.; Welton, T. *J. Org. Chem.* **2004**, *69*, 5986−5992.

10.1021/om0700157 CCC: $37.00 © 2007 American Chemical Society
Publication on Web 03/17/2007

Scheme 1

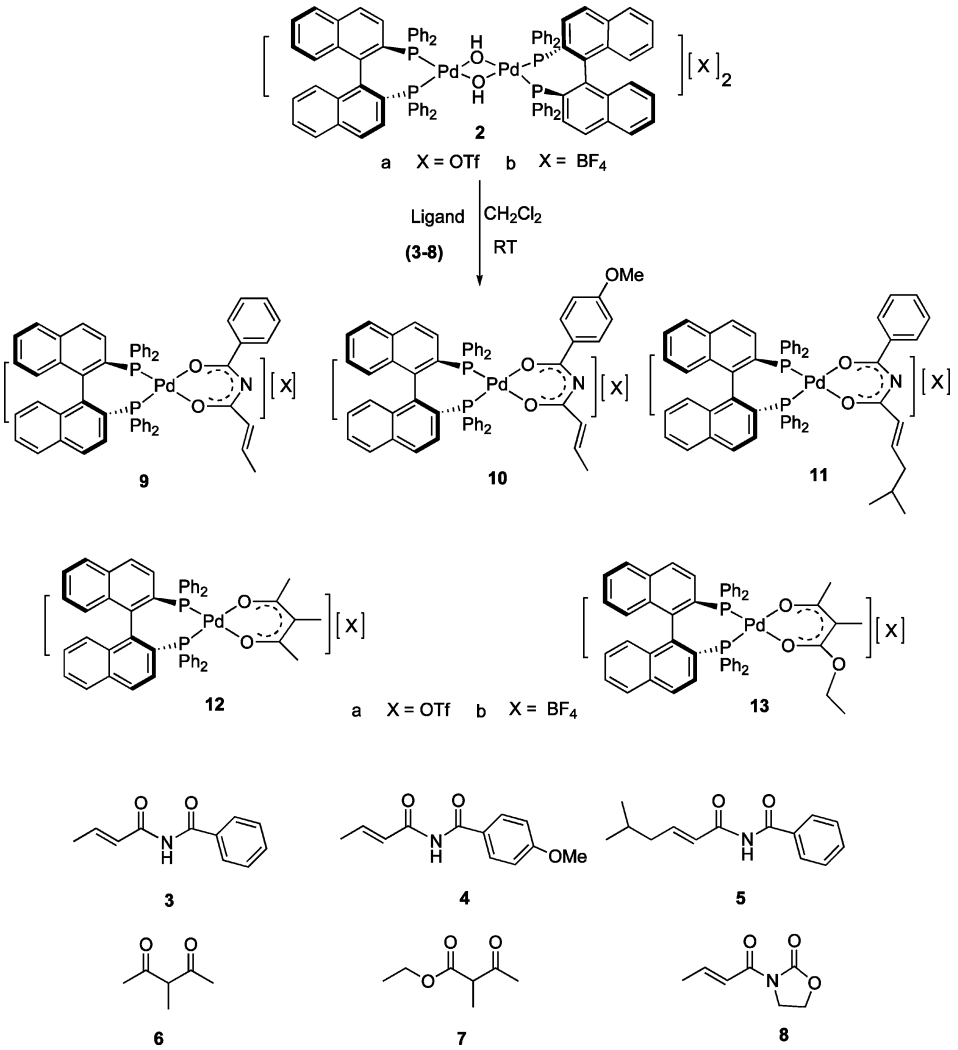

determining the nature of the product and/or the reaction kinetics.[9] Generally speaking, the anion may affect the solubility of the catalyst, accelerate or decelerate reactions, and occasionally improve reaction selectivity. Presumably the anion is not always "innocent" and may (a) block or actually take up a coordination position, (b) affect the cation via ion pairing, or (c) induce aggregation, i.e., significantly change the cation structure.

Increasingly, pulsed field gradient spin−echo (PGSE) diffusion measurements[15] are used to investigate possible ion pairing and/or aggregation of salts in solution.[16−26] The measurement of self-diffusion coefficients (*D* values) is especially useful when the cation and anion can be measured separately (e.g., via ^{1}H and ^{19}F NMR measurements), as their relative magnitudes can be revealing. In a given solvent, identical *D* values for the cation and anion suggest strong ion pairing[25] (in the absence of hydrogen bonding, encapsulation effects, etc.). The measured *D* values are in turn used to calculate a hydrodynamic radius (r_H) using the Stokes−Einstein relation (eq 1) by correcting for the solvent viscosity.

$$r_H = \frac{kT}{6\pi\eta D} \tag{1}$$

where *k* is the Boltzmann constant, η is the solution viscosity, and *T* is the temperature. Diffusion data, when combined with HOESY (or NOESY) measurements, assist in the understanding

(14) Faller, J. W.; Fontaine, P. P. *Organometallics* **2005**, *24*, 4132−4138.

(15) Price, W. S. *Concepts Magn. Reson.* **1997**, *9*, 299−336. Price, W. S. *Concepts Magn. Reson.* **1998**, *10*, 197−237. Stilbs, P. *Prog. Nucl. Magn. Reson. Spectrosc.* **1987**, *19*, 1.

(16) Jaing, Q.; Rüegger, H.; Venanzi, L. M. *Inorg. Chim Acta* **1999**, *290*, 64−79.

(17) Stahl, N. G.; Zuccaccia, C.; Jensen, T. R.; Marks, T. J. *J Am. Chem Soc.* **2003**, *125*, 5256−5257.

(18) Burini, A.; Fackler, J. P.; Galassi, R.; Macchioni, A.; Omary, M. A.; Rawashdeh-Omary, M. A.; Pietroni, B. R.; Sabatini, S.; Zuccaccia, C. *J. Am. Chem. Soc.* **2002**, *124*, 4570−4571.

(19) Binotti, B.; Macchioni, A.; Zuccaccia, C.; Zuccaccia, D. *Comments Inorg. Chem.* **2002**, *23*, 417−450.

(20) Zuccaccia, C.; Stahl, N. G.; Macchioni, A.; Chen, M. C.; Roberts, J. A.; Marks, T. J. *J. Am. Chem. Soc.* **2004**, *126*, 1448−1464.

(21) Ludwig, M.; Kadyrov, R.; Fiedler, H.; Haage, K.; Selke, R. *Chem.−Eur. J.* **2001**, *7*, 3298−3304.

(22) Fernández, I.; Martínez-Viviente, E.; Pregosin, P. S. *Inorg. Chem.* **2004**, *43*, 4555−4557. Martinez-Viviente, E.; Pregosin, P. S.: Vial, L.; Herse C.; Lacour, J. *Chem.−Eur. J.* **2004**, *10*, 2912−2918. Nama, D.; Kumar, P. G. A.; Pregosin, P. S.; Geldbach, T. J.; Dyson, P. J. *Inorg. Chim. Acta* **2006**, *359*, 1907−1911. M. Alajarin, M.; Pastor, A.; Orenes, R. A.; Martinez-Viviente, E.; Pregosin, P. S. *Chem.−Eur. J.* **2006**, *12*, 877−886.

(23) Brand, T.; Cabrita, E. J.; Berger, S. *Prog. Nucl. Magn. Reson. Spectrosc.* **2005**, *46*, 159−196.

(24) Cohen, Y.; Avram, L.; Frish, L. *Angew. Chem., Int. Ed.* **2005**, *44*, 520−554.

(25) Pregosin, P. S. *Prog. Nucl. Magn. Reson. Spectrosc.* **2006**, *49*, 261−288. Pregosin, P. S.; Kumar P. G. A.; Fernandez, I. *Chem. Rev.* **2005**, *105*, 2977−2998.

(26) Macchioni, A. *Chem. Rev.* **2005**, *105*, 2039−2073.

Table 1. ^{1}H and ^{13}C Chemical Shift Data[a] for Complex 14 and Oxazolidinone, 8

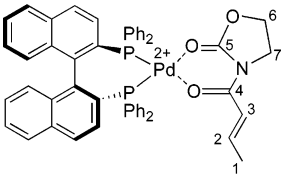

	δ ^{1}H	δ 13C
	8	
1	1.95	19.5
2	7.1−7.2	148.2
3	7.1−7.2	121.1
4		165.8
5		154.7
6	4.01	63.0
7	4.40	43.5
	14	
1	1.56	19.0
2	5.01	157.3
3	5.86	119.5
4		165.4
5		158.8
6	4.50	66.2
7	4.28	45.7

[a] δ ^{31}P = 37. 4, δ = 35.6, $^2J(^{31}P,^{31}P)$ = 9.5 Hz; 400 MHz, 203 K CD_2Cl_2.

of how ions interact and, specifically, the relative position of the anion with respect to the cation.[23,25,26]

Here we report the use of the bis-aquo complex **1**, $[Pd(H_2O)_2(BINAP)]_2(anion)_2$, **1a**,**b** (anion = **a**, $CF_3SO_3^-$; **b**, BF_4^-), containing racemic BINAP, to generate the bridging hydroxide species $[Pd(\mu\text{-OH})(BINAP)]_2(anion)_2$, **2a**,**b** (anion = **a**, $CF_3SO_3^-$; **b**, BF_4^-), which then reacts, cleanly, with the unsaturated N-imides **3**, **4**, and **5** or the 1,3-diketones **6** and **7** to afford a new set of monocationic Pd(II) BINAP complexes, **9** to **13**, in good to excellent yield (see Scheme 1). We also show that crotonyl oxazolidinone[(*E*)-3-but-2-enoyloxazolidin-2-one], **8**, coordinates to the Pd(BINAP) fragment via chelation of the two oxygen atoms to form a modest amount of the new, catalytically relevant, complex **14** (see eq 2). Finally, using PGSE diffusion

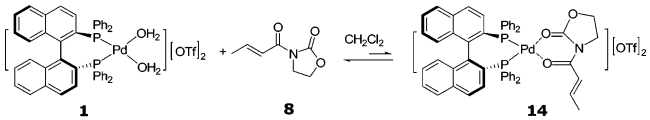

(2)

and HOESY NMR methods, we consider the nature of the ion pairing, with a view to recognizing possible steric effects in catalysis due to the position of the anion.

Results and Discussion

The well-known[5,7] diaquo complex $[Pd(H_2O)_2(BINAP)]_2(anion)_2$ represents a source of $[Pd(\mu\text{-OH})(BINAP)]_2(anion)_2$. Allowing these bridged hydroxy complexes, **2a**,**b**, to react with the appropriate unsaturated N-imides ligand precursors, **3**−**5**, or 1,3-diketones, **6** and **7**, in dichloromethane solution affords the monocationic Pd(II) BINAP complexes **9**−**11** and **12** and **13** (anion = **a**, $CF_3SO_3^-$; **b**, BF_4^-). The new chelating anions are generated using the bridging hydroxide ligand, and we note that related enolate complexes of palladium have been reported by several groups.[27−31]

Table 2. Bond Lengths (Å) and Bond Angles (deg) for Complex 12b

	12b·CH_2Cl_2		
Pd−O(2)	2.026(3)	Pd−O(1)	2.025(3)
Pd−P(1)	2.259(1)	Pd−P(2)	2.264(1)
P(1)−C(111)	1.811(4)	P(1)−C(121)	1.825(4)
P(1)−C(6)	1.838(4)	P(2)−C(221)	1.818(3)
P(2)−C(6′)	1.825(4)	P(2)−C(211)	1.822(4)
O(1)−C(2L)	1.292(5)	O(2)−C(4L)	1.281(5)
O(2)−Pd−O(1)	89.0(1)	O(2)−Pd−P(1)	89.23(9)
O(1)−Pd−P(1)	174.2(1)	O(2)−Pd−P(2)	177.3(1)
O(1)−Pd−P(2)	90.42(9)	P(1)−Pd−P(2)	91.57(3)
B−F (av)	1.4(3)	F−B−F (av)	107(1)
	12b		
Pd−O(2)	2.021(4)	Pd−O(1)	2.032(4)
Pd−P(1)	2.251(2)	Pd−P(2)	2.253(2)
P(1)−C(121)	1.802(6)	P(1)−C(111)	1.823(6)
P(2)−C(221)	1.819(6)	P(2)−C(211)	1.799(5)
P(1)−C(6)	1.834(5)	P(2)−C(6′)	1.837(8)
O(1)−C(2L)	1.275(7)	O(2)−C(4L)	1.276(7)
O(2)−Pd−O(1)	88.3(2)	O(2)−Pd−P(1)	88.5(1)
O(1)−Pd−P(1)	176.9(1)	O(2)−Pd−P(2)	171.4(1)
O(1)−Pd−P(2)	90.8(1)	P(1)−Pd−P(2)	92.32(5)
B−F (av)	1.25(3)	F−B−F (av)	108(2)

Solution Structures. The reaction of **2** with, for example, imide **4** produces 1 equiv of water via the deprotonation of the weakly acidic N*H* proton and the generation of Pd(II) salts **9**−**11**. The new products are readily identified via NMR spectroscopy. As an example, for the $CF_3SO_3^-$ complex **10a** in

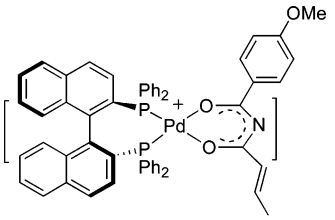

cation **10**

dichloromethane at room temperature, the $^{31}P\{^1H\}$ NMR spectrum shows an AB system, $^2J(PP)$ = 33.5 Hz, with the nonequivalent phosphorus nuclei, appearing at δ 35.5 and 35.1. In the ^{1}H NMR spectrum, one finds new resonances for the methyl and olefinic protons. Specifically, the C*H*$_3$ is found at δ 1.6, and the two olefinic resonances, $CH_3CH{=}CH$, as a strongly coupled spin system at δ 5.7−5.9. The corresponding ligand positions for **4** are δ 2.0, for the methyl signal, and δ 7.1−7.2 for the $CH_3CH{=}CH$ moiety. We believe that several of these low-frequency proton chemical shifts in **10a** arise from a mixture of anisotropic (P-phenyl on the BINAP proximate to the olefin) and chelation effects. Interestingly, all of the BINAP complexes reveal a rather broad aromatic proton resonance between δ 6 and 7. Earlier NMR studies[32,33] have shown that this signal is associated with restricted rotation of the P-axial phenyl groups.

(27) Braun, M.; Meier, T. *Synlett* **2006**, 661−676.

(28) Ketz, B. E.; Cole, A. P.; Waymouth, R. M. *Organometallics* **2004**, *23*, 2835−2837.

(29) Vicente, J.; Areas, A.; Fernandez-Hernandez, J. M.; Bautista, D.; Jones, P. G. *Organometallics* **2005**, *24*, 2516−2527.

(30) Gavrielatos, E.; Athanasellis, G.; Heaton, B. T.; Steiner, A.; Bickley, J. F.; Igglessi-Markopoulou, O.; Markopoulos, J. *Inorg. Chim. Acta* **2003**, *351*, 21−26.

(31) Tian, G. L.; Boyle, P. D.; Novak, B. M. *Organometallics* **2002**, *21*, 1462−1465.

(32) Trabesinger, G.; Albinati, A.; Feiken, N.; Kunz, R. W.; Pregosin, P. S.; Tschoerner, M. *J. Am. Chem. Soc.* **1997**, *119*, 6315.

(33) Nama, D.; Schott, D.; Pregosin, P. S.; Veiros, L. F.; Calhorda, M. J. *Organometallics* **2006**, *25*, 4596.

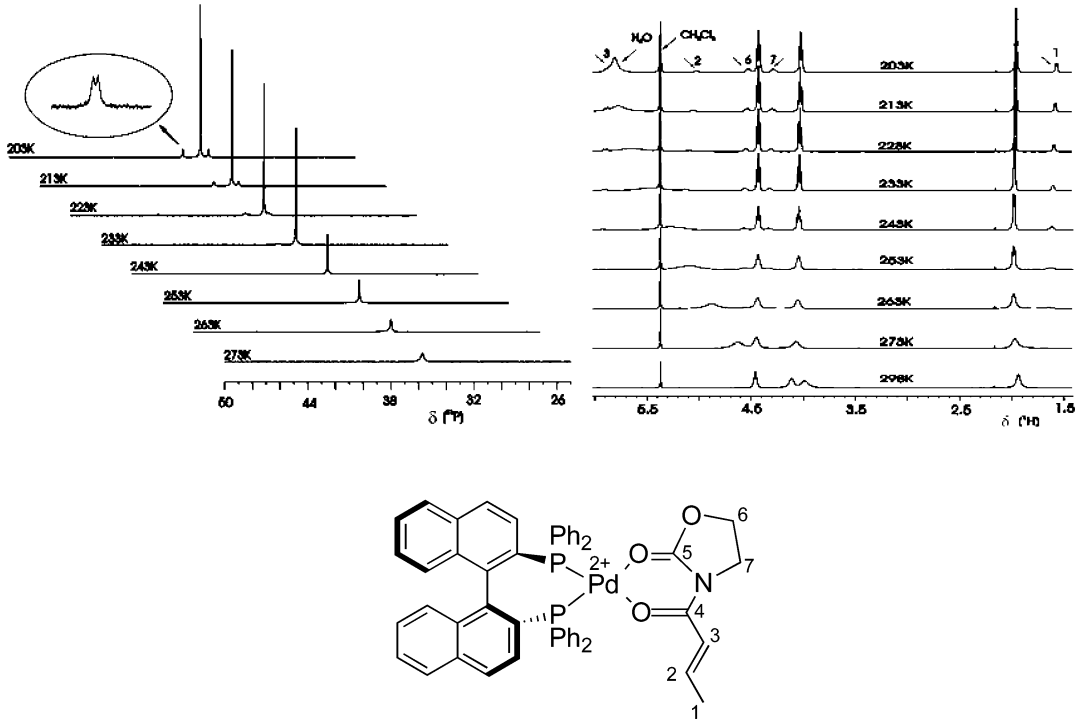

Figure 1. Variable-temperature ^{31}P (left) and ^{1}H (right) NMR spectra from a solution of complex **14**. The AX spin system in ^{31}P{^{1}H} spectra is visible (CD_2Cl_2, 20 mM, 500 MHz).

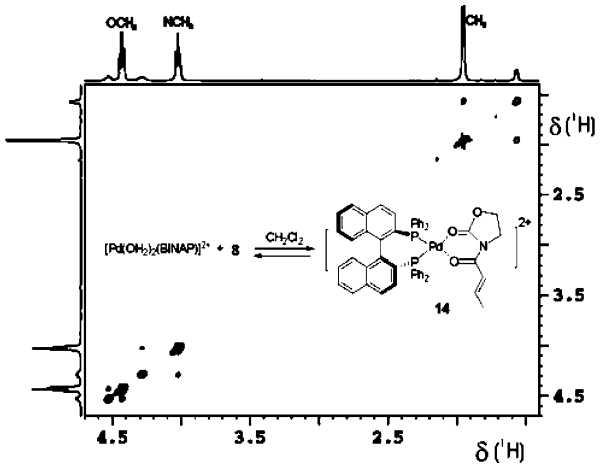

Figure 2. Section of ^{1}H,^{1}H NOESY spectrum of complex **14**, showing exchange between free ligand **8** and chelated ligand in complex **14** (CD_2Cl_2 500 MHz, 203 K).

Continuing, in the ^{13}C{^{1}H} NMR spectrum of **10a**, the two olefinic carbons, C2 and C3, are found at δ 145.9 (CH_3*C*H=CH) and 129.6 (CH_3CH=*C*H). These values do *not* correspond to a coordinated olefin, as the coordination chemical shifts, $\Delta\delta$ (=δ for **10a** − δ for **4**), are only −0.7 and 4.9 ppm, respectively.[49] It is useful to note that the deprotonation and complexation of **4** results in a small *low-frequency* (−0.7 ppm) change in the β-olefinic carbon chemical shift. This is not what one expects if this position is to be more electrophilic and thus more readily attacked by an amine nucleophile. A 2D ^{13}C,^{1}H long-range correlation reveals the two amide carbonyl carbons at δ 172.8 and 173.2. These chemical shift values are consistent with chelation of the anion of **4** to the metal through the oxygen atoms. Similar ^{31}P{^{1}H}, ^{1}H, and ^{13}C{^{1}H} NMR data were found in complexes **9** and **11**.

In a similar fashion, addition of ligand **6** or **7** to a dichloromethane solution of the bridged complexes **2a**,**b** (anion = **a**, CF_3SO_3; **b**, BF_4) results in the abstraction of the weakly acidic C*H* proton and the generation of Pd(II) enolate complexes **12** and **13**, respectively. For complex **13a**, in dichloromethane solution at room temperature, the ^{31}P{^{1}H} NMR spectrum shows an AX doublet, ^{2}J(PP) = 38 Hz, with the resonances appearing at δ 30.3 and 34.8. In the ^{1}H NMR spectrum the absence of doublet multiplicity associated with the central methyl group is consistent with the deprotonated and complexed ligand. Further, the OCH_2 moiety now appears as two diastereotopic CH_2 protons, δ 2.65 and 2.90, shifted to low frequency due to the proximate P-phenyl aromatic ring. In the ^{13}C{^{1}H} NMR spectrum, the central carbon, between the two carbonyl carbons, appears at δ 90.5, $\Delta\delta$ 29 ppm, and is no longer attached to a proton. The 2D ^{13}C,^{1}H long-range correlation reveals the two carbonyl carbons (*C*OMe, *C*OOC_2H_5) at δ 184.2 and 169.8, respectively. This same ^{13}C correlation allows one to assign the two, singlet, ^{1}H methyl groups of **13a** in that the signal at δ 1.70 reveals cross-peaks to *both* ^{13}C carbonyl resonances, via the two different ^{3}J(^{13}C,^{1}H) pathways.

NMR Characterization of Dicationic Complex 14. The addition of ligand **8** to the precursor complex [Pd(μ-OH)(BINAP)]$_2$(CF_3SO_3)$_2$, **2a**, in dichloromethane does not yield complex **14**. However, reaction of ligand **8** with the aquo

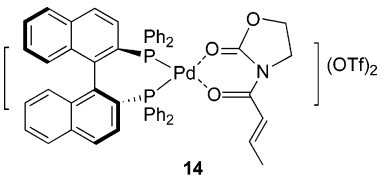

complex [Pd(H_2O)$_2$(BINAP)]$_2$(CF_3SO_3)$_2$, **1a**, in dichloromethane solution affords a mixture, which, via a low-temperature measurement, can be shown to contain ca. 16% of **14** plus unreacted starting material (see Figure 1). Both the ^{1}H and ^{31}P{^{1}H} spectra at room temperature gave broad resonances, suggesting dynamic behavior. The ^{31}P{^{1}H} NMR spectrum, which revealed a single broad peak at ca. δ 36.2 at room temperature, sharpens on cooling to 213 K, to reveal a major

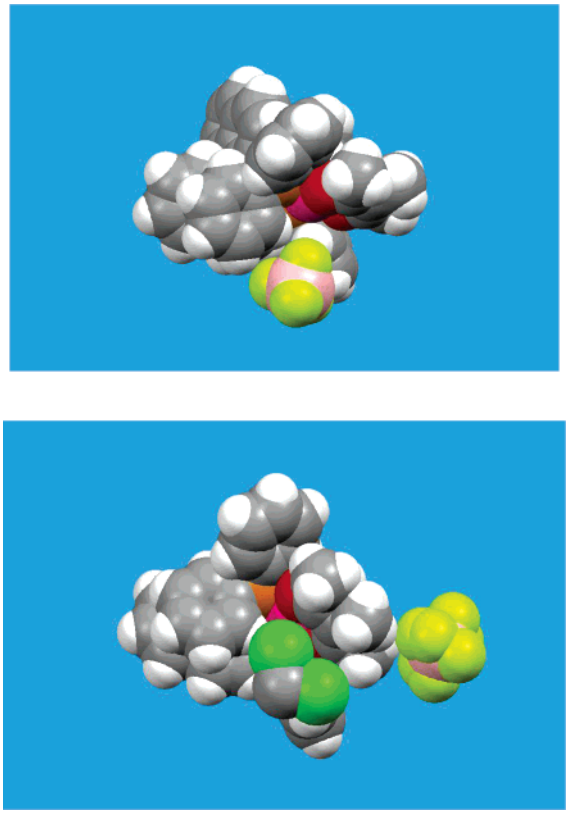

Figure 3. Views of the ion-paired (top, **12b**) and the solvent-separated (bottom, **12b**·CH_2Cl_2) salts.

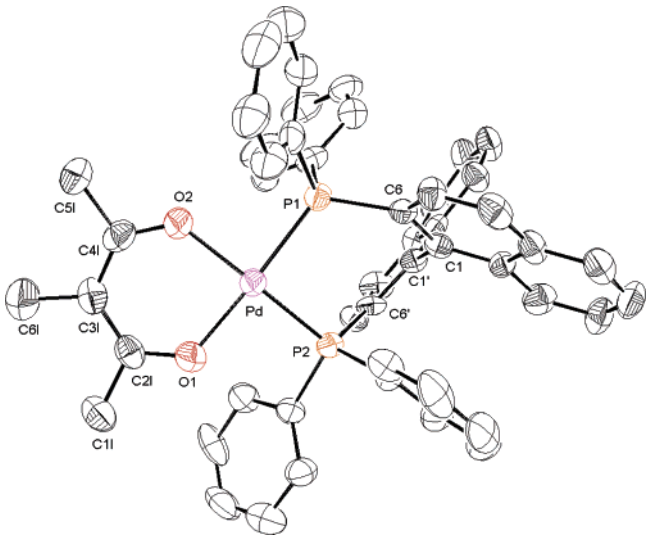

Figure 4. ORTEP view of the cation of **12b** with thermal ellipsoids drawn at the 50% probability level.

component (starting material), as a sharp singlet, along with a minor component as an AX spin system containing signals at ca. δ 35.5 and 37.5, $^2J(PP) = 9.5$ Hz.

Cooling of the solution to 203 K changes and resolves the broad ^{1}H NMR spectrum for this solution and reveals new proton resonances for the minor component, **14** (see Figure 1), and these chemical shift data are given in Table 1. We note that one of the olefinic resonances of **14** overlaps a water signal. The conventional $^{13}C\{^1H\}$ NMR spectrum and the 2D $^{13}C,^1H$ long-range correlation both reveal the two *C*H olefin carbons, C2 and C3, at δ 157.3 and 119.5, respectively (Table 1). These values, once again, are not consistent with olefin complexation. The C2 and C3 coordination chemical shifts, $\Delta\delta$ (= δ for **14** − δ for **8**), are +9.1 and −1.6 ppm, respectively; that is, complexation of **8** results in a very significant *high-frequency* (+9.1 ppm) change in the β-olefinic carbon chemical shift. These ^{13}C values are not consistent with direct olefin coordination, but the relatively large change for the β-olefinic carbon *is* what one expects if this carbon atom is to become more electrophilic through complexation and thus more readily attacked by a nucleophile. This is in contrast to what one finds for the ^{13}C data for **10**, noted above.

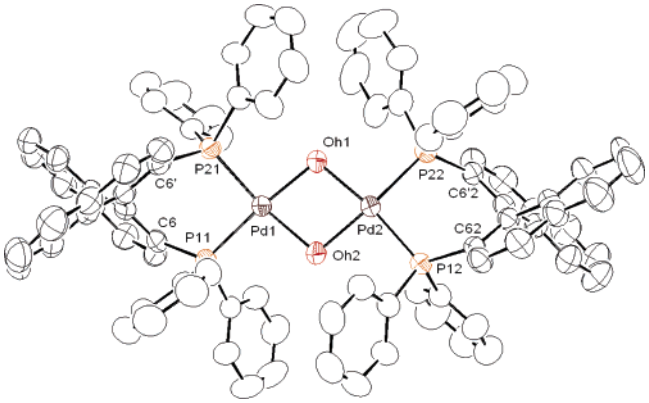

Figure 5. ORTEP view of the cation of **2a** with thermal ellipsoids drawn at the 50% probability level. Selected bond lengths (Å) and bond angles (deg): Pd(1)−OH1, 2.060(3), Pd(1)−OH2 2.080(3), Pd(1)−P(21) 2.225(1), Pd(1)−P(11) 2.233(1), Pd(2)−P(22) 2.226(1), Pd(2)−P(12) 2.232(1), Pd(1)−Pd(2) 3.1378(5), Pd(2)−OH1 2.062(3), Pd(2)−OH2 2.076(3), OH1−Pd(1)−OH2 79.7(1), OH1−Pd(1)−P(21) 93.3(1), OH2−Pd(1)−P(21) 171.3(1) OH1−Pd(1)−P(11) 170.8(1), OH2−Pd(1)−P(11) 95.1(1), P(21)−Pd(1)−P(11) 92.49(5), OH1−Pd(1)−Pd(2) 40.4(1), OH2−Pd(1)−Pd(2) 40.92(9), P(21)−Pd(1)−Pd(2) 130.99(3), P(11)−Pd(1)−Pd(2) 135.70(3), OH1−Pd(2)−OH2 79.8(1), OH1−Pd(2)−P(22) 95.0(1), OH2−Pd(2)−P(22) 171.2(1), OH1−Pd(2)−P(12) 171.1(1), OH2−Pd(2)−P(12) 92.2(1), P(22)−Pd(2)−P(12) 93.51(5).

From a phase-sensitive ^{1}H,^{1}H NOESY spectrum at 203 K, one finds exchange cross-peaks arising from the free oxazolidinone, **8**, and the chelated ligand in complex **14** (see Figure 2). The ease with which model salt **14** exchanges the complexed chelating ligand is clearly important for the mechanism of a catalytic reaction involving this type of substrate, since the addition product, once formed, must dissociate from the palladium to make room for the new substrate. While **14** represents only a minor component, it is obviously stable enough to be characterized and is clearly relevant to the palladium-catalyzed hydroamination chemistry noted in the Introduction.

X-ray Data. The solid-state structures of *two* separate forms of the BF_4^- complex, **12b** and **12b·CH_2Cl_2**, were determined by X-ray diffraction methods. Initially it was thought that two different materials had recrystallized; however as can been from Figure 3a (top), one form of the salt **12b** can be thought of as a tight ion pair, whereas the second form (Figure 3b, bottom) contains a dichloromethane solvent molecule, packed in approximately a fifth coordination position together with a relatively remote BF_4^- anion. Together these structures represent an *unprecedented example of a salt where the structures of both the solvent-stabilized cation and the tight ion-paired salt can be characterized*. This is, admittedly, a fortunate coincidence, in that the solution diffusion studies reveal only an average *D* value for the two ions; nevertheless, these solid-state data help us to envision structural aspects of these two extreme forms.

The two palladium cations are not very different, and Figure 4 shows a view of one of these. The local coordination geometry about the Pd atoms is distorted square planar, and the metric

Table 3. Diffusion Constants[a] and Radii[b] for Complexes 9 to 13 in CD_2Cl_2

	a ($CF_3SO_3^-$)						**b** (BF_4^-)					
	cation(^{1}H)			anion(^{19}F)			cation(^{1}H)			anion(^{19}F)		
compd	D	r_H	(r_H)	D	r_H	(r_H)	D	r_H	(r_H)	D	r_H	(r_H)
9	8.11	6.5	(7.1)	13.13	4.0	(5.0)	8.00	6.6	(7.1)	13.70	3.9	(4.8)
10	8.02	6.6	(7.1)	11.86	4.5	(5.2)	7.74	6.8	(7.3)	13.96	3.8	(4.8)
11	7.35	7.2	(7.7)	13.39	4.0	(4.9)	7.79	6.8	(7.3)	14.06	3.8	(4.8)
12	8.27	6.4	(7.0)	12.40	4.3	(5.1)	8.53	6.2	(6.8)	14.02	3.8	(4.8)
13	8.11	6.5	(7.1)	11.70	4.5	(5.3)	8.37	6.3	(6.9)	14.02	3.8	(4.8)

[a] 400 MHz, 2 mM; D values, 10^{-10} m^2 s^{-1}. [b] r_H values, Å; "c" corrected r_H values are in parentheses as suggested in ref 48. Estimated radii for the solvents $r_{vdw} = 2.49$ (CD_2Cl_2), $\eta(CH_2Cl_2) = 0.414 \times 10^{-3}$ kg m^{-1} s^{-1} at 299 K.

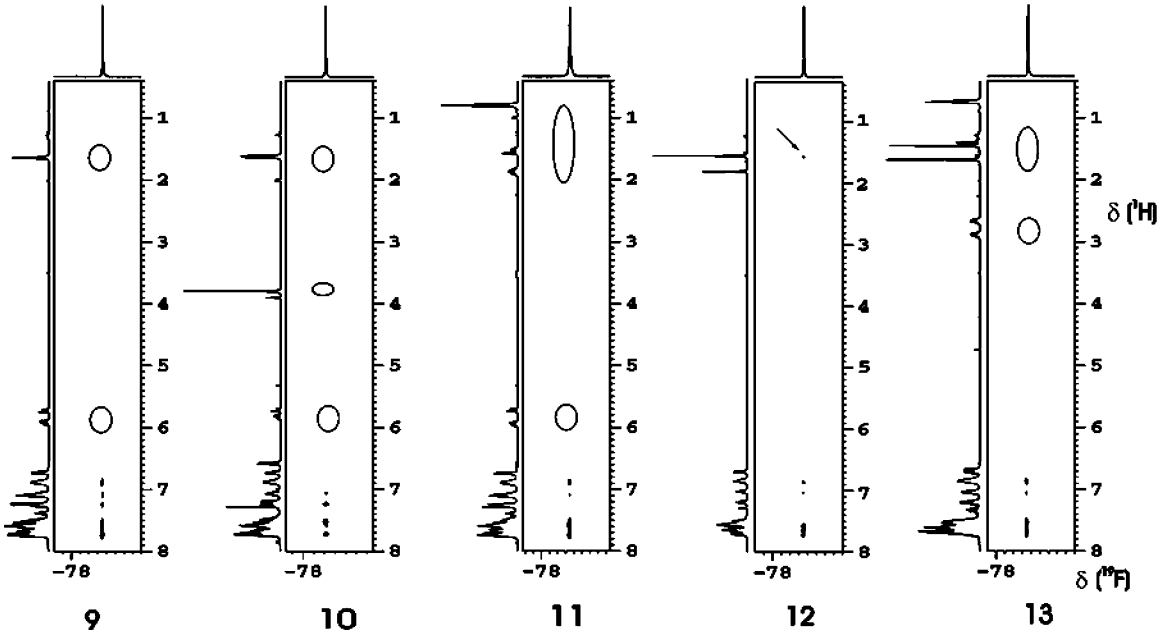

Figure 6. ^{1}H,^{19}F-HOESY spectra for the complexes **9a** to **13a** (CF_3SO_3 anion) in $CDCl_3$, all showing selective contacts primarily to the P-phenyl ring protons and not to the chelated anionic ligand. In complex **12**, one finds a weak contact (shown by arrow) to the methyl group (six protons). The empty circles indicate the absence of an NOE cross-peak (400 MHz, 298 K).

values for the two cations do not differ significantly (see Table 2). The various Pd-donor atom separations are normal,[34] as are the local coordination angles about the palladium atoms. However, we note that, to accommodate the square planar structure, the acetyl acetonate angles, O(1)−C(2L)−C(3L) = 126.1(4)° and O(2)−C(4L)−C(3L) = 127.1(4)°, in both cations are larger than the 120° values expected for sp^2 hybridization. As expected, the chiral pocket for the coordinated BINAP ligand reveals pseudoaxial and pseudoequatorial P-phenyl groups.[35−38]

There are two further modest structural differences between these two compounds: (1) The dihedral angle between the complexed acac ligand and the Pd,O1,O2,P1,P2 plane is 5.3(8)° for the CH_2Cl_2-solvated salt and 23.9° for the tight ion pair. Consequently, the coordinated acac is bent away from the closely positioned BF_4^- anion. (2) The Pd−P distances are slightly longer (>5σ) for the CH_2Cl_2-solvated salt than for the tight ion pair.

These do not represent major structural changes; however, they do indicate that the cation is responding to the two different environments.

In the course of our preparative work, crystals of the dinuclear μ-OH salt, **2a**, suitable for diffraction studies were obtained, and a view of this dication is given in Figure 5. The structure of the analogous *p*-tolyl salt has been reported by Sodeoka.[7b] The various metric parameters are rather standard, and we note that the four-membered Pd−O−Pd−O ring takes a distorted butterfly shape; that is, the ring is not flat. The dihedral angle between the two tetrahedrally distorted square planar Pd coordination planes is 18.6(1)°.

Diffusion Studies. PGSE diffusion data for the Pd(BINAP) $CF_3SO_3^-$ and BF_4^- salts, **9**−**13**, in dichloromethane solution are given in Table 3. The r_H values for cations fall in the range 6.2−7.2 Å (Table 3) and are in reasonable agreement with our earlier data on Pd BINAP complexes.[33] For **12b**, the r_H value of 6.2 Å is in excellent agreement with the r_{x-ray} value of 6.3

(34) Orpen, A. G.; Brammer, L.; Allen, F. H.; Kennard, O.; Watson, D. G.; Taylor, R. *J. Chem. Soc., Dalton Trans.* **1989**, S1.

(35) Ammann, C. J.; Pregosin, P. S.; Ruegger, H.; Albinati, A.; Lianza, F.; Kunz, R. W. *J. Organomet. Chem.* **1992**, *423*, 415−430. Pregosin, P. S.; Ruegger, H.; Salzmann, R.; Albinati, A.; Lianza, F.; Kunz, R. W. *Organometallics* **1994**, *13*, 83−90. Pregosin, P. S.; Ruegger, H.; Salzmann, R.; Albinati, A.; Lianza, F.; Kunz, R. W. *Organometallics* **1994**, *13*, 5040−5048. Barbaro, P.; Pregosin, P. S.; Salzmann, R.; Albinati, A.; Kunz, R. W. *Organometallics* **1995**, *14*, 5160. Drommi, D.; Nesper, R.; Pregosin, P. S.; Trabesinger, G.; Zurcher, F. *Organometallics* **1997**, *16*, 4268−4275. Magistrato, A.; Merlin, M.; Pregosin, P. S.; Rothlisberger, U.; Albinati, A. *Organometallics* **2000**, *19*, 3591.

(36) Zhang, X.; Mashima, K.; Koyano, K.; Sayo, N.; Kumobayashi, H.; Akutagawa, S.; Takaya, H. *J. Chem. Soc., Perkin Trans.* **1994**, 2309−2322.

(37) Oestreich, M.; Dennison, P. R.; Kodanko, J. J.; Overman, L. E. *Angew. Chem., Int. Ed.* **2001**, *40*, 1439−1442. Marshall, W. J.; Grushin, V. V. *Organometallics* **2003**, *22*, 555−562.

(38) Pregosin, P. S.; Rüegger, H. In *Comprehensive Coordination Chemistry II, Vol. 2*; McCleverty, A., Meyer, T. J., Eds.; Elsevier: Amsterdam, 2004; p 1. Pregosin, P. S.; Martinez-Viviente, E.; Kumar, P. G. A. *Dalton Trans.* **2003**, 4007, and references therein.

Table 4. Diffusion Constants[a] and Radii[b] for 9a−13a in THF-d_8 and $CDCl_3$ and, for 12, in CD_3CN

	a ($CF_3SO_3^-$)											
	THF						$CDCl_3$					
	cation(^{1}H)			anion(^{19}F)			cation(^{1}H)			anion(^{19}F)		
compd	D	r_H	(r_H)	D	r_H	(r_H)	D	r_H	(r_H)	D	r_H	(r_H)
9	6.43	7.4	(7.9)	9.25	5.1	(6.0)	5.66	7.2	(7.8)	5.96	6.9	(7.4)
10	6.28	7.6	(8.1)	9.30	5.1	(6.0)	5.53	7.4	(7.9)	6.46	6.3	(6.9)
11	6.06	7.8	(8.4)	8.93	5.3	(6.1)	5.26	7.8	(8.2)	6.08	6.7	(7.4)
12	6.78	7.0	(7.6)	9.24	5.1	(6.0)	5.82	7.0	(7.6)	6.30	6.5	(7.1)
13	6.55	7.3	(7.8)	9.43	5.0	(5.9)	5.88	7.0	(7.5)	6.29	6.5	(7.1)

	CD_3CN			
	cation(^{1}H)		anion(^{19}F)	
	D	r_H	D	r_H
12	10.22	6.2	23.86	2.7

[a] 400 MHz, 2 mM; D values, 10^{-10} m^2 s^{-1}. [b] r_H values, Å; "c" corrected r_H values as suggested in ref 48, are in parentheses. Estimated radii for the solvents: r_{vdw} = 2.68 (THF), r_{vdw} =2.60 ($CDCl_3$), $\eta(CHCl_3) = 0.534 \times 10^{-3}$ kg m^{-1} s^{-1} at 299 K, η(THF) = 0.461×10^{-3} kg m^{-1} s^{-1} at 299 K. $\eta(CH_3CN) = 0.345 \times 10^{-3}$ kg m^{-1} s^{-1} at 299 K, 2.60 ($CDCl_3$), $\eta(CHCl_3) = 0.534 \times 10^{-3}$ kg m^{-1} s^{-1} at 299 K, η(THF) = 0.461×10^{-3} kg m^{-1} s^{-1} at 299 K, $\eta(CH_3CN) = 0.345 \times 10^{-3}$ kg m^{-1} s^{-1} at 299 K.

Table 5. Experimental Data for the X-ray Diffraction Study of Compounds 2a·0.5(H_2O), 12b, and 12b·(CH_2Cl_2)

	2a·0.5(H_2O)	**12b**	**12b**·(CH_2Cl_2)
formula	$C_{90}H_{69}F_6O_{8.5}P_4Pd_2S_2$	$C_{50}H_{41}BF_4O_2P_2Pd$	$C_{51}H_{43}BCl_2F_4O_2P_2Pd$
mol wt	1800.24	928.98	1013.90
data coll. T, K	295(2)	295(2)	295(2)
diffractometer	Bruker APEX	Bruker SMART	Bruker APEX
cryst syst	monoclinic	orthorombic	triclinic
space group (no.)	$P2_1/c$ (14)	$Pna2_1$ (33)	$P\bar{1}$ (2)
a, Å	20.0621(5)	19.891(3)	11.560(4)
b, Å	18.7386(4)	16.856(2)	11.609(4)
c, Å	23.2203(5)	12.518(2)	18.806(6)
α, deg	90.	90.	78.198(7)
β, deg	96.572(1)	90	75.174(6)
γ, deg	90.	90.	73.210(7)
V, Å^3	8672.0(3)	4197.2(1)	2312(1)
Z	4	4	2
$\rho_{(calcd)}$, g cm^{-3}	1.379	1.470	1.456
μ, cm^{-1}	6.04	5.77	6.42
radiation	Mo Kα (graphite monochrom., λ = 0.71073 Å)		
θ range, deg	$1.49 < \theta < 26.09$	$2.03 < \theta < 21.36$	$1.85 < \theta < 25.99$
no. of indep data	17 073	4719	8988
no. of obsd reflns (n_o) [$\lvert F_o\rvert^2 > 2.0\sigma(\lvert F\rvert^2)$]	12 120	4196	7094
no. of params refined (n_v)	978	541	560
R_{int}	0.0506	0.0575	0.0375
R (obsd reflns)[a]	0.0616	0.0315	0.0515
R_w^2 (obsd reflns)[b]	0.1705	0.0726	0.1431
GOF[c]	1.031	1.012	1.018

[a] $R = \sum (\lvert F_o - (1/k)F_c\rvert)/\sum\lvert F_o\rvert$. [b] $R_w^2 = [\sum w(F_o^2 - (1/k)F_c^2)^2/\sum w\lvert F_o^2\rvert^2]$. [c] GOF $= [\sum w(F_o^2 - (1/k)F_c^2)^2/(n_o - n_v)]^{1/2}$.

Å found for the ion-paired structure and only slightly smaller than the r_{x-ray} value of 6.5 Å found for the dichloromethane-solvated species. The corresponding radii for the $CF_3SO_3^-$ anion, 4.0−4.5 Å, are somewhat larger than the values estimated for the solvated anion in methanol solution (ca. 3 Å[25,38]). Clearly, the anion and cation are not moving at an identical rate. The BF_4^- anion shows r_H values in the range 3.8−3.9 Å (Table 3), which are also a bit larger than for the isolated anion in methanol solution.[25,38] As in previous studies we assign these results to partial ion pairing in dichloromethane solution.

In THF solution the r_H values for the cations of the $CF_3SO_3^-$ salts, **9a** to **13a**, are larger and fall in the range 7.0−7.8 Å (Table 4), whereas those for the anion now span the range 5.0−5.3 Å. Ion pairing is usually more pronounced in THF than in dichloromethane,[25] and we suggest that this is reflected in these increased radii; however, the larger solvent THF will also contribute to the increase in the size of the cation r_H, relative to dichloromethane solutions. In any case, the r_H values for the cations and anions in THF solution suggest that these monocations are more strongly, but not completely, associated with the anions.

Continuing with the $CF_3SO_3^-$ salts, using $CDCl_3$ as solvent, the r_H values for cations are even larger and fall in the range 7.2−7.8 Å. The corresponding radii for the CF_3SO_3 anion, ca. 6.3−6.9 Å (Table 4), are now ca. 2 Å larger than in dichloromethane. These cation and anion r_H values suggest that the change of solvent from dichloromethane to THF and then to $CDCl_3$ has resulted in an increasingly tight ion pair. To contrast the $CDCl_3$ data, we have measured the diffusion for complex **12a** in CD_3CN, a much more polar solvent. As expected, the r_H value for the $CF_3SO_3^-$ anion, at 2.7 Å, approaches the value of the solvated anion.

A plot of the D value for the $CF_3SO_3^-$ anion versus dielectric constant of the solvent ($CHCl_3$ (4.8) < THF (7.6) < CH_2Cl_2 (8.9) < CH_3CN (37.5)) is not linear. However, the graph (not shown) clearly shows that the diffusion constant of the anion

increases (faster motions, less ion pairing) with an increase in dielectric constant of the solvent.

^{1}H,^{19}F-HOESY NMR Experiments. To further explore the ion paring, and to place the cation in three-dimensional space, relative to the anion, ^{1}H,^{19}F-HOESY spectra for **9a**−**13a** in chloroform solution were measured, and these are shown in Figure 6 . In all of these spectra the strongest cross-peaks arise due to the fluorine spins of the $CF_3SO_3^-$ anion interacting with P-phenyl (probably *ortho*) aromatic protons of the complexed BINAP. There are almost no contacts to either the chelating N-imide or the acetylacetonate. [There is a weak contact to the strongest methyl signal in **12**. The P-phenyl *ortho* aromatic protons of the complexed BINAP can be partially assigned via a ^{31}P,^{1}H COSY correlation.]

Consequently, we believe that the anion is (a) approaching the positive metal and phosphorus centers via a pathway that brings it closest to the P-phenyl groups and (b) avoiding the region of the negatively charged chelating ligands. The illustration below offers two possible pathways of approach. It is not necessary that the anion (indicated as a red ball) approach from a "vertical" position (dotted arrow), as this is not sterically favored.

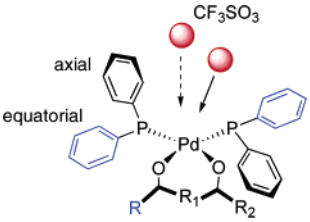

Conclusions

The Pd(BINAP) dication, **14**, postulated by Hii, in connection with the enantioselective Pd-catalyzed hydroamination reaction, clearly exists in solution and can be characterized at low temperature. It is not the major component of the mixture; however, its dynamic nature is consistent with the ease with which a possible product could be eliminated from the palladium moiety to allow the next substrate molecule to complex.

The new Pd complexes, **9**−**13**, might be generated in a catalytic solution containing a labile Pd(II)(BINAP) moiety, a diketone such as **6**, and a base. These conditions are fulfilled in a number of literature reports. However, their relative stability and the ^{13}C data for the olefinic carbons suggest that these may not be important in the palladium-catalyzed reactions, in agreement with a suggestion by Sodeoka.[7a] However, a related *Ru-enolate* has recently been suggested as an active intermediate in an asymmetric Michael addition reaction.[39]

As expected, the ion pairing in **9**−**13** is strongly solvent dependent, but, even in chloroform solution, where one finds the largest amount of ion pairing, there is no reason to believe that the ion pair would hinder attack of, for example, a nucleophile on the double bond of the complexed enolate, since the counteranion prefers to remain remote from the coordinated chelated anion.

Together, the structures of the two forms of the acetyl acetonate BF_4^- complex, **12b**, provide a rare structural picture of a tight ion pair versus a solvent-separated analogue. Moving the anion closer to the metal affects the cation structure.

Experimental Section

General Comments. All air-sensitive manipulations were carried out under a nitrogen atmosphere. All solvents were dried over appropriate drying agents, distilled under nitrogen. Deuterated solvents were dried by distillation over molecular sieves and stored under nitrogen. The ligands *rac*-BINAP (Strem), silver salts (Aldrich), and 1,3-diketones 3-methyl-2,4-dione, **6**, ethyl 2-methylacetoacetate, **7**, and (*E*)-3-but-2-enoyloxazolidin-2-one, **8** (Acros Organics), were purchased from commercial sources and used as received. The dichloro-metal complex $PdCl_2L_2$, L_2 = racemic BINAP, and the α,*β*-unsaturated N-imides (**3**, **4**, and **5**) were synthesized according to the literature.[40] ^{1}H, ^{31}P, ^{13}C, and ^{19}F NMR spectra were recorded with Bruker DPX-250, 300, 400, and 500 MHz spectrometers at room temperature unless otherwise noted. Elemental analysis and mass spectra were performed at ETH Zürich.

Crystallography. Crystals of [Pd(*rac*-BINAP)(CH_3−C(O)−C(CH_3)−C(O)−CH_3)](BF_4), **12b**, suitable for X-ray diffraction were obtained from a dichloromethane/hexane solution. In the same crystallization batch, crystals with two different colors (red and yellow, respectively) and crystal habits were present. Thus data were collected for both; one turned out to be the expected compound (**12b**) and the other a solvento complex (**12b**·CH_2Cl_2). The two crystals belong to different space groups with completely different molecular packings.

Dark yellow crystals of [Pd(*μ*-OH)(BINAP)]$_2$(CF_3SO_3)$_2$, **2a**, were obtained from dichloromethane/ether solution. The crystals were mounted on Bruker diffractometers, equipped with CCD detectors, for the unit cell and space group determinations. Selected crystallographic and other relevant data are listed in Table 5 and in the Supporting Information.

Data were corrected for Lorentz and polarization factors with the data reduction software SAINT[41] and empirically for absorption using the SADABS program.[42] The structures were solved by direct and Fourier methods and refined by full matrix least-squares[43] (the function minimized being $\sum[w(F_o^2 - 1/kF_c^2)^2]$). For all structures, no extinction correction was deemed necessary. The scattering factors used, corrected for the real and imaginary parts of the anomalous dispersion, were taken from the literature.[44] All calculations were carried out by using the PC version of the programs WINGX,[45] SHELX-97,[43] and ORTEP.[46]

Structural Study of [Pd(*rac*-BINAP)(CH_3−C(O)−C(CH_3)−C(O)−CH_3)](BF_4), 12b. The space group was unambiguously determined from the systematic absences, while the cell constants were refined by least-squares, at the end of the data collection. The data were collected by using *ω* scans, in steps of 0.5°. For each of the 1440 collected frames, the counting time was 30 s. The least-squares refinement was carried out using anisotropic displacement parameters for all non-hydrogen atoms. The BF_4 anion is disordered, as can be seen from the large ADPs, preventing an accurate determination of the geometry. The final Fourier difference map did not reveal any significant feature. The contribution of the hydrogen atoms, in their calculated positions, C−H = 0.96 Å, B(H) = $aB(C_{bonded})$ Å^2 (a = 1.3 or 1.5 for methyl groups), was included in the refinement using a riding model.

Structural Study of [Pd(*rac*-BINAP)(CH_3−C(O)−C(CH_3)−C(O)−CH_3)](BF_4)·CH_2Cl_2, 12b·CH_2Cl_2. The space group was assumed to be $P\bar{1}$ and confirmed by the successful refinement. The

(39) Althaus, M.; Bonaccorsi, C.; Mezzetti, A.; Santoro, F. *Organometallics* **2006**, *25*, 3108−3110.
(40) Myers, J. K.; Jacobsen, E. N. *J. Am. Chem. Soc.* **1999**, *121*, 8959−8960.
(41) *BrukerAXS, SAINT*, Integration Software; Bruker Analytical X-ray Systems: Madison, WI, 1995.
(42) Sheldrick, G. M. *SADABS*, Program for Absorption Correction; University of Göttingen: Göttingen, Germany, 1996.
(43) Sheldrick, G. M. *SHELX-97*, Structure Solution and Refinement Package; Universität Göttingen, 1997.
(44) *International Tables for X-ray Crystallography*; Wilson, A. J. C., Ed.; Kluwer Academic Publisher: Dordrecht, The Netherlands, 1992; Vol. C.
(45) Farrugia, L. J. *J. Appl. Crystallogr.* **1999**, *32*, 837.
(46) Farrugia, L. J. *J. Appl. Crystallogr.* **1997**, *30*, 565.

cell constants were refined by least-squares, at the end of the data collection. The data were collected by using ω scans, in steps of 0.3°. For each of the 1860 collected frames, the counting time was 30 s. The least-squares refinement was carried out using anisotropic displacement parameters for all non-hydrogen atoms of the cation.

The BF_4^- group, again, showed positional disorder of the fluorine atoms. Two different orientations for the F atoms were clearly shown in the difference Fourier maps; split F atoms, in the two orientations, were used to model the disordered anion and refined isotropically (refined sof 0.5 for each site). The Fourier difference maps also showed the presence of a clathrated CH_2Cl_2 molecule, which was refined anisotropically. The H atoms were included in the refinement as described above.

Structural Study of [Pd(μ-OH)(BINAP)]$_2$(CF_3SO_3)$_2$·0.5H_2O, 2a·0.5H_2O. The space group was unambiguously determined from the systematic absences. The values of the cell parameters were refined at the end of the data collection. The data were collected by using ω scans, in steps of 0.3°. For each of the 1878 collected frames, the counting time was 30 s. The least-squares refinement of the cation was carried out using anisotropic displacement parameters for all non-hydrogen atoms. Fourier difference maps revealed the presence of a water molecule that was refined anisotropically with an sof of 0.5 for each site. The two triflate counterions are disordered. Anisotropic refinement of only one cation led to a significantly better fit (as judged from a Hamilton's test[47]); the other was refined isotropically. The contribution of the hydrogen atoms, in their calculated positions (C−H = 0.96 Å, B(H) = 1.3B(C_{bonded}) Å^2), was included in the refinement using a riding model.

Diffusion Measurements. All of the PGSE measurements were carried out using the stimulated echo pulse sequence and performed on a Bruker Avance spectrometer, 400 MHz, equipped with a microprocessor-controlled gradient unit and a multinuclear inverse probe with an actively shielded Z-gradient coil. The shape of the gradient pulse was rectangular, and its length was 1.75 ms. The gradient strength was incremented in 4% steps from 4% to 60%, so that 12−15 points could be used for regression analysis. The time between midpoints of the gradients was 167.75 ms, and gradient recovery time was set to 100 μs for all experiments. All the diffusion ^{1}H spectra were acquired using 16K points, 16 transients, a 5 s relaxation delay, and a 1.5 s acquisition time. All the ^{19}F spectra were acquired using 16K points, 16 or 8 transients, a relaxation delay of 5 times T_1 (approximately 15−20 s), and a 4 s acquisition time. Both the ^{1}H and ^{19}F diffusion experiments were processed using Bruker software with an exponential multiplication (EM) window function and a line broadening of 1.0 HZ. The measurements were carried out without spinning at a set temperature of 299 K within the NMR probe. As indicated in Table 3 and 4, diffusion values were measured on 2 mM CD_2Cl_2, $CDCl_3$, and d_8-THF solutions. Cation diffusion rates were measured using the ^{1}H signal from the aromatic protons of BINAP and/or from chelated ligand signals. Anion diffusion was obtained from the ^{19}F resonances. The error in the D values is thought to be ±0.06. The solvent viscosities used for the calculation of r_H were 0.414, 0.534, and 0.461 for CD_2Cl_2, $CDCl_3$, and d_8-THF, respectively.

NOE Measurements. The ^{1}H,^{1}H NOESY NMR experiments were acquired by the standard three-pulse sequence (noesyph) using a 1 s relaxation delay and 600 ms of mixing time on a Bruker 500 MHz spectrometer at a set temperature of 203 K (DS 16, DE 6.0 μs, pulse width (PW): F1 4496.4 Hz, F2 4496.4 Hz). The ^{19}F,^{1}H-HOESY NMR experiments were acquired by the standard four-pulse sequence (invhoesy) and carried out using a doubly tuned TXI probe on a 400 MHz spectrometer at a set temperature of 298 K. A mixing time of 800 ms was used, and 16 scans were taken for each of the 512 t_1 increments recorded. The delay between increments was set to 1 s (DS 4, DE 7.14 μs, pulse width (PW): F1 3601.1 Hz, F2 1132.2 Hz).

(*E*)-*N*-(2-Phenylacetyl)but-2-enamide (3). ^{1}H NMR (CD_2Cl_2, 400 MHz, 25 °C): δ 2.00 (t, 3H, J = 6.4 Hz), 7.2 (m, 3H), 7.5−7.9 (m, 5H), 8.86 (s, 1H). ^{13}C{^{1}H} NMR (CD_2Cl_2, 100 MHz, 25 °C): δ 18.7 (CH_3), 55.9 (OCH_3), 124.6 ($CH_3CH{=}CH$), 128.1 (Ar), 129.2 (Ar), 133.4 (Ar), 133.6 (Ar), 147.0 ($CH_3CH{=}CH$), 166.2 (ArC=O), 167.4 (NC=O).

(*E*)-*N*-(2-(4-Methoxyphenyl)acetyl)but-2-enamide (4). ^{1}H NMR (CD_2Cl_2, 400 MHz, 25 °C): δ 2.00 (t, 3H, J = 5.6 Hz), 7.1 (m, 2H), 7.0 (d, 2H, J = 8.8 Hz), 7.8 (d, 2H, J = 8.8 Hz), 8.5 (s, 1H). ^{13}C{^{1}H} NMR (CD_2Cl_2, 100 MHz, 25 °C): δ 18.7 (CH_3), 55.9 (OCH_3), 114.5 (Ar), 124.7 ($CH_3CH{=}CH$), 125.6 (Ar), 130.2 (Ar), 146.6 ($CH_3CH{=}CH$), 165.4 (ArC=O), 167.3 (NC=O).

(*E*)-5-Methyl-*N*-(2-phenylacetyl)hex-2-enamide (5). ^{1}H NMR (CD_2Cl_2, 300 MHz, 25 °C): δ 1.00 (d, 3H, J = 8.8 Hz), 1.85 (m, 1H), 2.2 (t, 2H, J = 9.2 Hz), 7.1−7.9 (m, 7H), 8.42 (s, 1H). ^{13}C{^{1}H} NMR (CD_2Cl_2, 100 MHz, 25 °C): δ 22.5 (CH_3)$_2$, 28.3 (CH(CH3)$_2$), 42.1 (CH_2CH(CH3)$_2$), 124.2 ($CH_2CH{=}CH$), 128.1 (Ar), 129.2 (Ar), 133.4 (Ar), 133.7 (Ar), 150.8 ($CH_2CH{=}CH$), 166.2 (ArC=O), 167.4 (NC=O).

3-Methyl-2,4-dione (6). ^{1}H NMR (CD_2Cl_2, 250 MHz, 25 °C): δ 1.3 (d, 3H, J = 7.0 Hz), 2.20 (s, 3H), 3.67 (q, 1H, J = 7.0 Hz), 2.1 (s, 3H). ^{13}C{^{1}H} NMR (CD_2Cl_2, 62.9 MHz, 25 °C): δ 12.3 ($CHCH_3$), 28.6 ($CH_3C{=}O$), 61.5 ($CHCH_3$), 190.4 (s).

Ethyl 2-methylacetoacetate (7). ^{1}H NMR (CD_2Cl_2, 400 MHz, 25 °C): δ 1.28 (t, 3H, J = 7.2 Hz), 1.31 (d, 3H, J = 7.2 Hz), 2.23 (s, 3H), 3.52 (q, 1H, J = 7.2 Hz), 4.20 (q, 2H, J = 7.2 Hz). ^{13}C{^{1}H} NMR (CD_2Cl_2, 62.9 MHz, 25 °C): δ 12.8 ($CHCH_3$), 14.2 (CH_3CH_2), 28.6 ($CH_3C{=}O$), 53.9 ($CHCH_3$), 61.6 (CH_3CH_2), 170.8 ($C_2H_5C{=}O$), 203.9 ($CH_3C{=}O$).

[3-[(*E*)-2-Butenoyl]-1,3-oxazolidin-2-one] (8). ^{1}H NMR (CD_2Cl_2, 500 MHz, 203 K): δ 1.95 (d, 3H, J = 6.4 Hz), 4.01 (t, 2H, J = 8.3 Hz), 4.4 (t, 2H, J = 7.9 Hz), 7.1−7.2 (m, 2H). ^{13}C{^{1}H} NMR (CD_2Cl_2, 125 MHz, 203 K): δ 19.5 (CH_3CH), 43.5 (NCH_2), 63.0 (OCH_2), 121.1($CH{=}CHC{=}O$), 148.2 (CH_3CH), 154.7 ($OC{=}O$), 165.8 (NC=O).

[Pd(*rac*-BINAP)($C_{11}H_{10}NO_2$)][CF_3SO_3] (9a). To 1 equiv of [Pd-

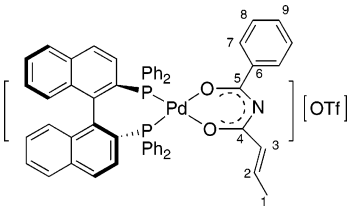

(μ-OH)(*rac*-BINAP)]$_2$[CF_3SO_3]$_2$ (99.5 mg, 1790.36 g mol^{-1}, 55.6 × 10^{-3} mol) was added 2 equiv of the $C_{11}H_{11}NO_2$ (21 mg, 189 g mol^{-1}, 111.1 × 10^{-3} mol) in dichloromethane. The reaction mixture was stirred at 25 °C for 3 h. The resulting yellow solution was reduced *in vacuo*. The resulting residue was washed with Et_2O to afford [$C_{56}H_{42}P_2O_5NF_3PdS$], **9a** (yield: 100 mg, 0.094 mol 84%). CHN % {found (calcd)} [Pd(*rac*-BINAP)($C_{11}H_{10}NO_2$)][CF_3SO_3]·H_2O: C {62.07 (61.95)}, H {4.10 (4.03)}, N {1.29 (1.29)}. ^{1}H NMR (CD_2Cl_2, 400 MHz, 25 °C): δ 1.65 (d, 3H, H1, J = 6.5 Hz), 5.7−6.0 (m, 2H, H2/3), 6.7−7.9 (m, 37H). ^{31}P{^{1}H} NMR (CD_2Cl_2, 161 MHz, 25 °C): δ 33.5 ppm (d, AB spin, J = 32 Hz). ^{19}F NMR (CD_2Cl_2, 282 MHz, 25 °C): δ −78.8 (s). ^{13}C{^{1}H} NMR (CD_2Cl_2, 100 MHz, 25 °C): δ 18.2 (s, C1), 128.1 (s, C8), 128.8 (s, C9), 129.6 (s, C3), 130.1 (s, C7), 135.4 (s, C6), 146.5 (s, C2), 173.3 (d, C5, $^1J_{CN}$ = 3 Hz), 174.1 (d, C4, $^1J_{CN}$ = 3 Hz), 120−180 ppm. (BINAP) MS (ESI; m/z): M$^+$ 916.2, [M − $C_{11}H_{10}NO_2$]$^+$ 729.0.

(47) Hamilton, W. C. *Acta. Crystallogr.* **1965**, *17*, 502.

(48) Zuccaccia, D.; Macchioni, A. *Organometallics* **2005**, *24*, 3476−3486.

(49) Mann, B. E.; Taylor, B. F. *^{13}C NMR Data for Organometallic Compounds*; Academic Press: London, 1981.

[Pd(*rac*-BINAP)($C_{12}H_{12}NO_3$)][CF_3SO_3] (10a). To 1 equiv of

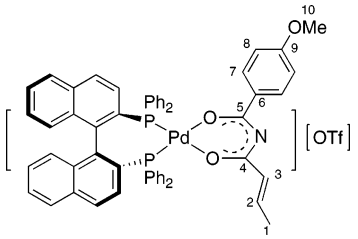

[Pd(μ-OH)(*rac*-BINAP)]$_2$[CF_3SO_3]$_2$ (2.8 mg, 1790.36 g mol^{-1}, 23.9 $\times$ 10^{-3} mol) was added 2 equiv of the $C_{12}H_{13}NO_3$(10.6 mg, 219.2 g mol^{-1}, 48.3 $\times$ 10^{-3} mol) in dichloromethane. The reaction mixture was stirred at 25 °C for 3 h. The resulting yellow solution was reduced *in vacuo*. The resulting residue was washed with Et_2O to afford **10a** (yield: 45 mg, 0.0410 mol, 85%). CHN % {found (calcd)} [Pd(*rac*-BINAP)($C_{12}H_{12}NO_3$)][CF_3SO_3]·H_2O: C {61.48 (61.89)}, H {4.17 (4.11)}, N {1.26 (1.30)}. ^{1}H NMR (CD_2Cl_2, 400 MHz, 25 °C): δ 1.63 (d, 3H, H1 J = 6.0 Hz), 3.8 (s, 3H, H10), 5.7−5.9 (m, 2H, H2/3), 6.6−7.9 (m, 36H). ^{31}P{^{1}H} NMR (CD_2Cl_2, 161 MHz, 25 °C): δ 33.5 ppm (d, AB spin, $^2J_{PP}$ = 33 Hz). ^{19}F NMR (CD_2Cl_2, 282 MHz, 25 °C): δ −78.8 (s). ^{13}C{^{1}H} NMR (CD_2Cl_2, 100 MHz, 25 °C): δ 18.2 (s, C1), 55.6 (s, C10), 113.4 (s, C8), 127.9 (s, C6), 129.6 (s, C3), 132.5 (s, C7), 135.4 (s, C6), 145.9 (s, C2), 164.7 (s, C9), 172.8 (d, C5), 173.2 (d, C4, $^1J_{CN}$ = 3 Hz), 120−180 ppm. (BINAP) MS (ESI; *m*/*z*): M$^+$ 946.3.

[Pd(*rac*-BINAP)($C_{14}H_{16}NO_2$)][CF_3SO_3] (11a). To 1 equiv of

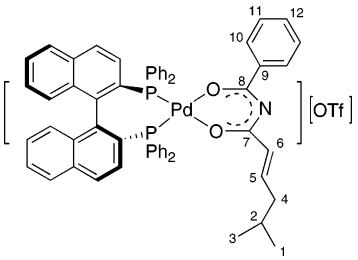

[Pd(μ-OH)(*rac*-BINAP)] $_2$[CF_3SO_3]$_2$ (35 mg, 1790.36 g mol^{-1}, 19.5 $\times$ 10^{-3} mol) was added 3 equiv of the $C_{14}H_{17}NO_2$ (13.6 mg 231.13 g mol^{-1}, 58.8 $\times$ 10^{-3} mol) in dichloromethane. The reaction mixture was stirred at 25 °C for 3 h. The resulting yellow solution was reduced *in vacuo*. The resulting residue was washed with Et_2O to afford **11a** (yield: 58 mg, 89%). ^{1}H NMR (CD_2Cl_2, 400 MHz, 25 °C): δ 0.81 (t, 6H, J = 5.2 Hz, H1,3), 1.53 (m, 1H, H2), 1.9 (m, 2H, H4), 5.3−6.0 (m, 2H, H5,6), 6.7−7.8 (m, 37H). ^{31}P{^{1}H} NMR (CD_2Cl_2, 161 MHz, 25 °C): δ 33.6 ppm (d, $^2J_{pp}$ = 33 Hz), 34.7 (d, $^2J_{pp}$ = 33 Hz). ^{19}F NMR (CD_2Cl_2, 282 MHz, 25 °C): δ −79.1(s). ^{13}C{^{1}H} NMR (CD_2Cl_2, 100 MHz, 25 °C): δ 22.4 (s, C3), 22.6 (s, C1), 28.0 (s, C4), 41.9 (s, C2), 129.5 (s, C6), 150.1 (s, C5), 173.3 (s, C8), 174.0 (s, C7) 120−180 ppm. (BINAP) MS (ESI; *m*/*z*): M$^+$ 871.2, [M − $C_{14}H_{16}NO_2$]$^+$ 729.0.

[Pd(*rac*-BINAP)($C_6H_9O_2$)][CF_3SO_3] (12a). To 1 equiv of [Pd-

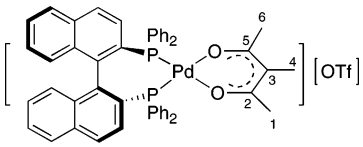

(μ-OH)(*rac*-BINAP)]$_2$[CF_3SO_3]$_2$ (50 mg, 1790.36 g mol^{-1}, 27.9 $\times$ 10^{-3} mol) was added 2 equiv of the $C_6H_{10}O_2$ (6.5 μL, 144.14 g mol^{-1}, 0.981 g cm^{-3}) in dichloromethane. The reaction mixture was stirred at 25 °C for 3 h. The resulting yellow solution was reduced *in vacuo*. The resulting residue was washed with Et_2O to afford **12a** (yield: 48 mg, 0.048 mol, 86%). CHN % [Pd(*rac*-BINAP)($C_6H_9O_2$)][CF_3SO_3]·H_2O: {found (calcd)} C {61.73 (60.86)}, H {4.27 (4.23)}. ^{1}H NMR (CD_2Cl_2, 400 MHz, 25 °C): δ 1.58 (s, 6H, H1,6), 1.8 (s, 3H, H4), 6.7−7.8 (m, 32H). ^{31}P{^{1}H} NMR (CD_2Cl_2, 161 MHz, 25 °C): δ 31.9 ppm (s). ^{19}F NMR (CD_2Cl_2, 282 MHz, 25 °C): δ −78.8 (s). ^{13}C{^{1}H} NMR (CD_2Cl_2, 100 MHz, 25 °C): δ 16.0 (s, C4), 26.9 (t, C1/C6, J_{CP} = 5 Hz), 104.3 (s, C3), 185.5 (s, C2/C5), 120−180 ppm. (BINAP) MS (ESI; *m*/*z*): M$^+$ 841.1, [M − $C_6H_9O_2$]$^+$ 729.0.

[Pd(*rac*-BINAP)($C_7H_{11}O_3$)][CF_3SO_3] (13a). To 1 equiv of [Pd-

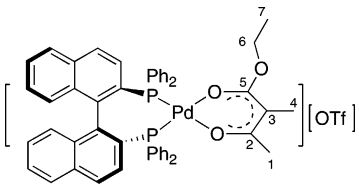

(μ-OH)(*rac*-BINAP)] $_2$[CF_3SO_3]$_2$ (40.7 mg, 1790.36 g mol^{-1}, 24.4 $\times$ 10^{-3} mol) was added 2 equiv of the $C_7H_{12}O_3$ (7.0 μL, 144.17 g mol^{-1}, 1.019 g cm^{-3}) in dichloromethane. The reaction mixture was stirred at 25 °C for 3 h. The resulting yellow solution was reduced *in vacuo*. The resulting residue was washed with Et_2O to afford **13a** (yield: 42 mg, 0.045 mol, 89%). CHN % {found (calcd)} [Pd (*rac*-BINAP)($C_7H_{11}O_3$)][CF_3SO_3]·H_2O: C {60.10 (60.02)}, H {4.49 (4.46)}. ^{1}H NMR (CD_2Cl_2, 400 MHz, 25 °C): δ 0.75 (t, 3H, H7, J = 7.1 Hz), 1.47 (s, 3H, H1), 1.7 (s, 3H, H4), 2.7−2.9 (m, 2H, H6), 6.7−7.8 (m, 32H). ^{31}P{^{1}H} NMR (CD_2Cl_2, 161 MHz, 25 °C): δ 30.4 ppm (d, $^2J_{pp}$ = 38 Hz), 34.7 (d, $^2J_{pp}$ = 38 Hz). ^{19}F NMR (CD_2Cl_2, 282 MHz, 25 °C): δ −154 (s). ^{13}C-{^{1}H} NMR (CD_2Cl_2, 100 MHz, 25 °C): δ 13.0 (s, C4), 14.3 (s, C7), 25.8 (s, C1), 60.9 (s, C6), 90.5 (s, C3), 169.8 (s, C2), 184.2 (s, C5), 120−180 ppm. (BINAP) MS (ESI; *m*/*z*): M$^+$ 871.2, [M − $C_7H_{11}O_3$]$^+$ 729.0.

[Pd(*rac*-BINAP)($C_{11}H_{10}NO_2$)][BF_4] (9b). To 1 equiv of [Pd-(μ-OH)(*rac*-BINAP)]$_2$[BF_4]$_2$ (33.1 mg, 1665.84 g mol^{-1}, 19.8 $\times$ 10^{-3} mol) was added 2.1 equiv of the $C_{11}H_{11}NO_2$ (6.7 mg, 189 g mol^{-1}, 35.4 $\times$ 10^{-3} mol) in dichloromethane. The reaction mixture was stirred at 25 °C for 3 h. The resulting yellow solution was reduced *in vacuo*. The resulting residue was washed with Et_2O to afford [$C_{55}H_{42}BF_4NO_2P_2Pd$], **9b** (yield: 31 mg, 87%). ^{1}H NMR (CD_2Cl_2, 400 MHz, 25 °C): δ 1.65 (d, 3H, H1, J = 6.8 Hz), 5.7−6.0 (m, 2H, H2/3), 6.7−7.9 (m, 37H). ^{31}P{^{1}H} NMR (CD_2Cl_2, 161 MHz, 25 °C): δ 33.5 ppm (d, AB spin, J = 32 Hz). ^{19}F NMR (CD_2Cl_2, 282 MHz, 25 °C): δ −153.9 (s). ^{13}C{^{1}H} NMR (CD_2Cl_2, 100 MHz, 25 °C): δ 18.0 (s, C1), 128.1 (s, C8), 128.9 (s, C9), 129.6 (s, C3), 130.1 (s, C7), 135.4 (s, C6), 146.5 (s, C2), 173.3 (d, C5, $^1J_{CN}$ = 3 Hz), 174.0 (d, C4, $^1J_{CN}$ = 3 Hz), 120−180. (BINAP) MS (ESI; *m*/*z*): M$^+$ 916.2, [M − $C_{11}H_{10}NO_2$]$^+$ 729.0.

[Pd(*rac*-BINAP)($C_{12}H_{12}NO_3$)][BF_4] (10b). To 1 equiv of [Pd-(μ-OH)(*rac*-BINAP)]$_2$[BF_4]$_2$ (51 mg, 1665.84 g mol^{-1}, 30.6 $\times$ 10^{-3} mol) was added 2 equiv of the $C_{12}H_{13}NO_3$ (13.4 mg, 219.2 g mol^{-1}, 61.1 $\times$ 10^{-3} mol) in dichloromethane. The reaction mixture was stirred at 25 °C for 3 h. The resulting yellow solution was reduced *in vacuo*. The resulting residue was washed with Et_2O to afford **10b** (yield: 55 mg, 0.0410 mol, 87%). ^{1}H NMR (CD_2Cl_2, 400 MHz, 25 °C): δ 1.63 (d, 3H, H1 J = 6.8 Hz), 3.8 (s, 3H, H10), 5.7−5.9 (m, 2H, H2/3), 6.6−7.9 (m, 36H). ^{31}P{^{1}H} NMR (CD_2Cl_2, 161 MHz, 25 °C): δ 33.5 (d, AB spin, $^2J_{PP}$ = 33 Hz). ^{19}F NMR (CD_2Cl_2, 282 MHz, 25 °C): δ −153.9 (s). ^{13}C{^{1}H} NMR (CD_2Cl_2, 100 MHz, 25 °C): δ 17.9 (s, C1), 55.8 (s, C10), 113.4 (s, C8), 127.9 (s, C6), 129.6 (s, C3), 132.5 (s, C7), 135.4 (s, C6), 145.8 (s, C2), 164.2 (s, C9), 172.8 (d, C5), 173.2 (d, C4, $^1J_{CN}$ = 3 Hz), 120−180. (BINAP) MS (ESI; *m*/*z*): M$^+$ 946.3.

[Pd(*rac*-BINAP)($C_{14}H_{16}NO_2$)][BF_4] (11b). To 1 equiv of [Pd-(μ-OH)(*rac*-BINAP)]$_2$[BF_4]$_2$ (52.3 mg, 1665.84 g mol^{-1}, 31.4 $\times$ 10^{-3} mol) was added 3 equiv of the $C_{14}H_{17}NO_2$ (21.8 mg, 231.13 g mol^{-1}, 94.3 $\times$ 10^{-3} mol) in dichloromethane. The reaction mixture was stirred at 25 °C for 3 h. The resulting yellow solution

was reduced *in vacuo*. The resulting residue was washed with Et_2O to afford **11b** (yield 54 mg, 82%). ^1H NMR (CD_2Cl_2, 400 MHz, 25 °C): δ 0.81 (t, 6H, $J = 5.2$ Hz), 1.53 (m, 1H), 1.9 (m, 2H), 5.3−6.0 (m, 2H), 6.7−7.8 (m, 37H). $^{31}P\{^1H\}$ NMR (CD_2Cl_2, 161 MHz, 25 °C): δ 33.6 (d, AB spin, $^2J_{PP} = 32$ Hz). ^{19}F NMR (CD_2Cl_2, 282 MHz, 25 °C): δ −154.0 (s). $^{13}C\{^1H\}$ NMR (CD_2Cl_2, 100 MHz, 25 °C): δ 22.4 (s, C3), 22.6 (s, C1), 28.0 (s, C4), 41.9 (s, C2), 129.5 (s, C6), 150.1 (s, C5), 173.3 (s, C8), 174.0 (s, C7), 120−150. (BINAP) MS (ESI; *m/z*): M^+ 871.2, $[M - C_{14}H_{16}NO_2]^+$ 729.0.

[Pd(*rac*-BINAP)($C_6H_9O_2$)][BF_4] (12b). To 1 equiv of [Pd(μ-OH)(*rac*-BINAP)]$_2$[BF_4]$_2$ (54.8 mg, 1665.84 g mol^{-1}, 27.9 × 10^{-3} mol) was added 2 equiv of the $C_6H_{10}O_2$ (7.7 μL, 144.14 g mol^{-1}, 0.981 g cm^{-3}) in dichloromethane. The reaction mixture was stirred at 25 °C for 3 h. The resulting yellow solution was reduced *in vacuo*. The resulting residue was washed with Et_2O to afford **12b** (yield: 50 mg, 0.053 mol, 96%). CHN % {found (calcd)} [Pd(*rac*-BINAP)($C_6H_9O_2$)][BF_4]: C {63.92 (64.57)}, H {4.60 (4.55)}. ^1H NMR (CD_2Cl_2, 400 MHz, 25 °C): δ 1.57 (s, 6H), 1.82 (s, 3H), 6.7−7.8 (m, 32H). $^{31}P\{^1H\}$ NMR (CD_2Cl_2, 161 MHz, 25 °C): δ 31.9 (s). ^{19}F NMR (CD_2Cl_2, 282 MHz, 25 °C): δ −154 (s). $^{13}C\{^1H\}$ NMR (CD_2Cl_2, 100 MHz, 25 °C): δ 15.9 (s, C4), 26.6 (t, C1/C6, $J_{CP} = 5$ Hz), 104.3 (s, C3), 185.3 (s, C2/C5), 120−180. (BINAP) MS (ESI; *m/z*): M^+ 840.9, $[M - C_6H_9O_2]^+$ 729.0.

[Pd(*rac*-BINAP)($C_7H_{11}O_3$)][BF_4] (13b). To 1 equiv of [Pd(μ-OH)(*rac*-BINAP)]$_2$[BF_4]$_2$ (67.0 mg, 1665.84 g mol^{-1}, 40.2 × 10^{-3} mol) was added 2 equiv of the $C_7H_{12}O_3$ (11.4 μL, 144.17 g mol^{-1}, 1.019 g cm^{-3}) in dichloromethane. The reaction mixture was stirred at 25 °C for 3 h. The resulting yellow solution was reduced *in vacuo*. The resulting residue was washed with Et_2O to afford **13b** (yield: 47 mg, 0.045 mol, 86%). ^1H NMR (CD_2Cl_2, 400 MHz, 25 °C): δ 0.75 (t, 3H, H7, $J = 7.1$ Hz), 1.47 (s, 3H, H1), 1.7 (s, 3H, H4), 2.7−2.9 (m, 2H, H6), 6.7−7.8 (m, 32H). $^{31}P\{^1H\}$ NMR (CD_2Cl_2, 161 MHz, 25 °C): δ 30.4 (d, $^2J_{pp} = 38$ Hz), 34.7 (d, $^2J_{pp} = 38$ Hz). ^{19}F NMR (CD_2Cl_2, 282 MHz, 25 °C): δ −154 (s). $^{13}C\{^1H\}$ NMR (CD_2Cl_2, 100 MHz, 25 °C): δ 13.0 (s, C4), 14.3 (s, C7), 25.8 (s, C1), 60.9 (s, C6), 90.5 (s, C3), 169.9 (s, C2), 184.0 (s, C5), 120−180. (BINAP) MS (ESI; *m/z*): M^+ 871.2, $[M - C_7H_{11}O_3]^+$ 729.0.

[Pd(*rac*-BINAP)($C_7H_9NO_3$)][CF_3SO_3]$_2$ (14). ^1H NMR (CD_2Cl_2, 500 MHz, 203 K): δ 1.56 (d, 3H, H1, $J = 6.8$ Hz), 4.28 (m, 2H, H7), 4.5 (t, 2H, H6, $J = 9.8$ Hz), 5.0 (m, 1H, H2), 5.86(d, 1H, H3). $^{13}C\{^1H\}$ NMR (CD_2Cl_2, 125 MHz, 203 K): δ 19.0 (s, C1), 45.7 (d, C7), 66.2 (s, C6), 119.5 (s, C3), 157.3 (s, C2), 158.8 (s, C5), 165.4 (s, C4). $^{31}P\{^1H\}$ NMR (CD_2Cl_2, 202 MHz, 203 K): δ 37.4 (d, $J = 9.5$ Hz), 35.6 (d, $J = 9.5$ Hz).

Crystallographic data have been deposited at the Cambridge Crystallographic Data Centre (CCDC Nos. 624568 (**2a**), 624569 (**12b**), and 624570 (**12b**·CH_2Cl_2)).

Acknowledgment. P.S.P. thanks the Swiss National Science Foundation and the ETH Zurich for support, as well as the Johnson Matthey Organization for the loan of palladium salts. A.A. thanks MURST for a grant (PRIN 2004).

Supporting Information Available: Experimental details and a full listing of crystallographic data, including tables of positional and isotropic equivalent displacement parameters, anisotropic displacement parameters, calculated positions of the hydrogen atoms, bond distances, bond angles, and torsional angles for compounds **2a**, **12b**, and **12b**·CH_2Cl_2. This material is available free of charge via the Internet at http://pubs.acs.org.

OM0700157